NLO QCD correction to $e^{-}p \rightarrow e^{-}Hj/\nu_{e}Hj$ processes at LHeC collider

Biswajit Das

The Institute of Mathematical Sciences, Chennai, India

in collaboration with **Pramod Sharma** and **Ambresh Shivaji**, IISER Mohali

ASWMSA, NISER, Jan 19, 2024

Overview

Motivation : $e^- p \to e^- Hj/\nu_e Hj$

- Higgs boson (125GeV) has been discovered at the LHC in 2012.
- Although the Higgs boson properties are compatible with SM, we still do not have conclusive evidence of new physics.
- Higgs production processes will help to provide the stringent bounds on Higgs couplings and validate the Higgs mechanism.
- *pp*-colliders have large amounts of QCD background; hence it is difficult to put stringent bounds on Higgs couplings.
- We consider Higgs boson production processes at the proposed $e^- p$-colliders, in particular at LHeC for their relatively cleaner background.

CMS bounds [1]

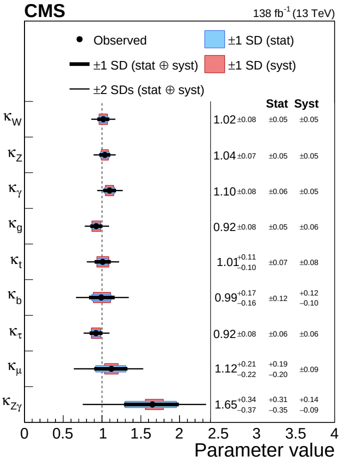

Figure: CMS bounds on Higgs couplings in κ-framework.

[1] Nature 607, 60–68 (2022)

Motivation

Colliders	CME (TeV)	Processes	x-section(pb)
pp	14	$pp \to hjj$	3.7
ILC	1	$e^+e^- \to e^+e^-h$ $e^+e^- \to \nu_e\bar{\nu}_e h$	0.007 0.21
CLIC	3	$e^+e^- \to e^+e^-h$ $e^+e^- \to \nu_e\bar{\nu}_e h$	0.0006 0.5
LHeC	1.98	$e^-p \to e^-hj$ $e^-p \to \nu_e hj$	0.05 0.2

- Sufficiently large cross-section as compared to e^+e^- colliders.
- e^--energy can be varied in a range of $50 - 200$ GeV with the proton beam of 7 TeV at LHeC.
- No automation for higher order correction for eP collision.
- NLO QCD correction can add significant contributions to these processes.

Feynman diagrams :

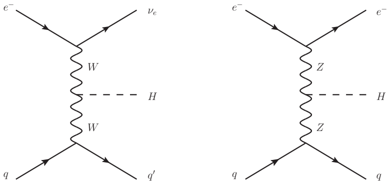

Figure: Tree-level diagrams for CC and NC processes.

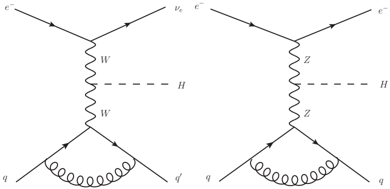

Figure: QCD one-loop diagrams for CC and NC processes.

Feynman diagrams :

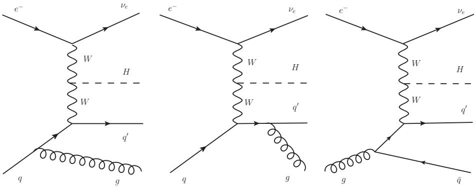

Figure: QCD real emission diagrams for CC process.

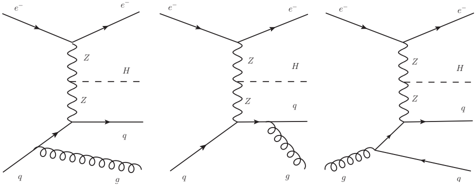

Figure: QCD real emission diagrams for NC process.

Coupling Order :

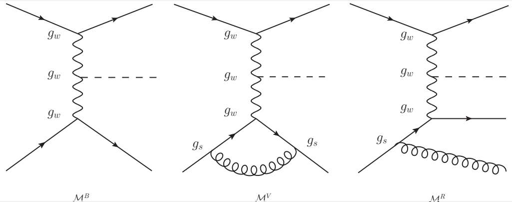

$$\mathcal{M}^B \sim \mathcal{O}(g_w^3)\,, \quad \mathcal{M}^V \sim \mathcal{O}(g_s^2 g_w^3)\,, \quad \mathcal{M}^R \sim \mathcal{O}(g_s g_w^3)\,.$$

$$\Longrightarrow \mid \mathcal{M} \mid^2_m \sim \mid \mathcal{M}^B \mid^2 + 2.Re\left[\mathcal{M}^B . \mathcal{M}^{V^*}\right]\,, \quad \mid \mathcal{M} \mid^2_{m+1} \sim \mid \mathcal{M}^R \mid^2$$

$$\therefore \sigma^T = \sigma^B(\alpha_w^3) + \sigma^V(\alpha_w^3 \alpha_s) + \sigma^R(\alpha_w^3 \alpha_s)$$

Amplitude computation :

- We compute born-level (LO and NLO) helicity amplitudes by using spinor helicity formalism at the matrix element level.
- We calculate virtual amplitude in t'Hooft-Veltman (HV) regularization scheme where only the loop part has been computed in d-dimension, and the rest part has been computed in 4-dimension.

Virtual Amplitude :

$$\mathcal{M}^V = \frac{\alpha_s}{2\pi} . \frac{(4\pi)^\epsilon}{\Gamma(1-\epsilon)} . C_F . \left(\frac{\mu^2}{t}\right)^\epsilon . \left\{ -\frac{1}{\epsilon^2} - \frac{3}{2\epsilon} - 4 + \mathcal{O}(\epsilon) \right\} \times \mathcal{M}^B$$

- The phase-space integral is being done with the Monte-Carlo package called AMCI. The package AMCI is based on the VEGAS algorithm.
- We use the parallel virtual machine (PVM) to compute the phase-space integrals across the nodes.

UV divergence

- QCD does not renormalize electroweak coupling at one-loop.
- We do not need to add any CT for the NLO QCD correction to this process.
- The poles in virtual amplitudes are completely IR.

Infrared Singularity :

- As gluon (massless gauge-boson) is being exchanged between two massless quarks, the virtual diagram is collinear as well as soft divergent.
- The real emission diagrams are also IR divergent in soft and collinear regimes.
- The real emission and renormalized virtual amplitudes are both divergent in 4-dimension, but the sum of these two is finite.
- Two types of real emission sub-processes can contribute to σ^{NLO}: 1. $e^- q \to lHjj$ and 2. $e^- g \to lHjj$.
- The final state 4-body phase-space integral is very hard to calculate analytically. Instead, we implement a subtraction scheme, where we can perform phase-space integral in 4-dimensional for real emission diagrams.

Dipole Subtraction scheme

- We implement the Catani-Seymour dipole subtraction scheme for IR singularity cancellation.
- A local counterterm ($d\sigma^A$) is being added to virtual diagrams and subtracted from real emission diagrams. This local counterterm has the same pointlike behavior as real emission diagram at collinear and soft regions.

$$\begin{aligned}\sigma^{NLO} &= \int_{m+1}\left[d\sigma^R - d\sigma^A\right] + \int_m \left[d\sigma^V - \int_1 d\sigma^A\right] \\ &= \int_{m+1}\left[\left(d\sigma^R\right)_{\epsilon=0} - \left(\Sigma_{ijk}\mathcal{D}_{ij,k}\right)_{\epsilon=0}\right] + \int_m \left[d\sigma^V - d\sigma^B \otimes I\right]_{\epsilon=0}\end{aligned}$$

- In this process, we have quarks (antiquarks) as the initial and final state partons.

Dipole Subtraction scheme

The insertion operator :

$$I = \frac{\alpha_s}{2\pi}.\frac{(4\pi)^\epsilon}{\Gamma(1-\epsilon)}.2C_F.\left(\frac{\mu^2}{t}\right)^\epsilon.\left\{\frac{1}{\epsilon^2}+\frac{3}{2\epsilon}+5-\frac{\pi^2}{2}+\mathcal{O}(\epsilon)\right\}$$

- This **I**-term cancels all IR poles $(\frac{1}{\epsilon^2},\frac{1}{\epsilon})$ from $d\sigma^V$.
- There are two dipole terms associated with each real emission sub-process. The dipole terms are $\mathcal{D}_k^{ai}$ and $\mathcal{D}_{ij}^{a}$.
- These dipole terms exhibit the same singular behavior as $d\sigma^R$ in collinear and soft regions.
- There is also collinear-subtraction counterterm which is the finite remnant after leftover collinear singularities absorbed in PDF.

Input parameters and Scale choice

- Input parameter:

$$\mathrm{M}_W = 80.379\,\mathrm{GeV}, \quad \Gamma_W = 2.085\mathrm{GeV}$$
$$\mathrm{M}_Z = 91.1876\,\mathrm{GeV}, \quad \Gamma_Z = 2.4952\,\mathrm{GeV}$$
$$G_\mu = 1.16638 \times 10^{-5}\mathrm{GeV}^2, \quad \alpha = \frac{\sqrt{2}}{\pi} G_\mu M_W^2 \left(1 - \frac{M_W^2}{M_Z^2}\right)$$

- We consider the following dynamical scale for PDF evolution and running of strong coupling.

$$\mu_R = \mu_F = \mu_0 = \frac{1}{3}\left(p_{T,l} + \sqrt{p_{T,H}^2 + M_H^2} + p_{T,j}\right)$$

- We compute the scale uncertainty by varying $\mu_{R/F}$ in between $0.5\mu_0 \leq \mu_{R/F} \leq 2\mu_0$.

Results : NC and CC

Collider Energy : $E_e = 140$ GeV, $E_p = 7$ TeV (CME= 1.98 TeV)

Process $e^- p \to$	σ_0 (fb)	σ_{qcd}^{NLO} (fb)	RE (%)
$e^- Hj$	$44.70^{+1.97\%}_{-1.86\%}$	$49.08^{+0.41\%}_{-0.53\%}$	9.80
$\nu_e Hj$	$214.31^{+2.30\%}_{-2.13\%}$	$237.59^{+0.89\%}_{-0.72\%}$	10.86

Here $\sigma_{qcd}^{NLO} = \sigma^0 + \sigma^V + \sigma^I + \sigma^{PK} + \sigma^{DSR}$. Where DSR stands for dipole subtracted real emission.

The relative enhancement is defined as $RE = \left(\frac{\sigma_{qcd}^{NLO} - \sigma_0}{\sigma_0}\right) \times 100$.

p_T and η -distributions : $e^- p \to e^- Hj$

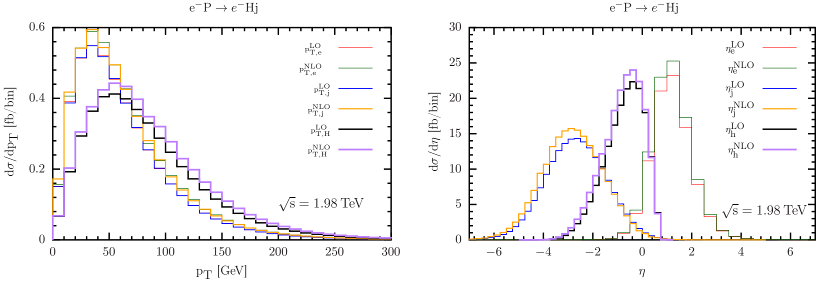

Figure: The LO and NLO differential cross section distribution with respect to transverse momenta (p_T) and rapdity(η).

Invariant-mass distributions : $e^- p \to e^- Hj$

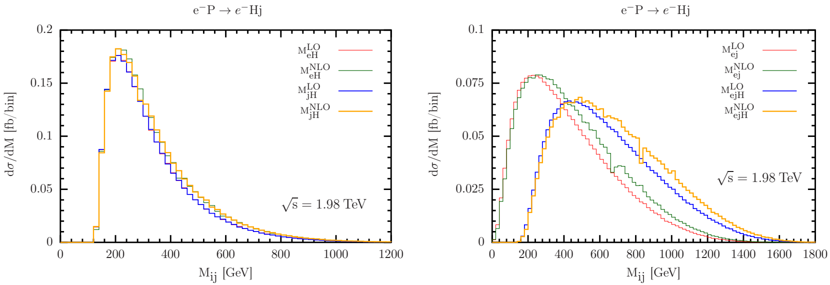

Figure: The LO and NLO differential cross section distribution with respect to invariant masses ($M_{ij/ijk}$).

p_T and η -distributions : $e^- p \to \nu_e Hj$

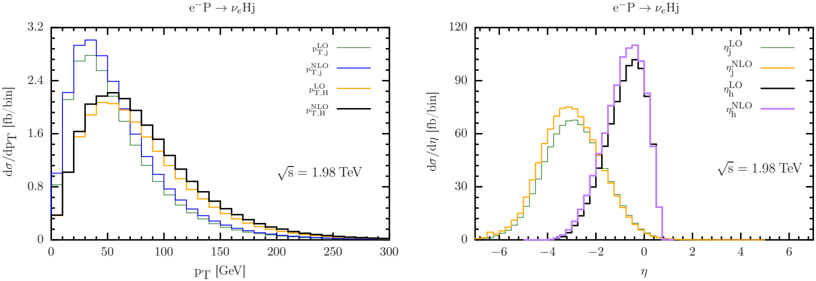

Figure: The LO and NLO differential cross section distribution with respect to transverse momentums (p_T) and rapidity (η).

Invariant-mass distributions : $e^{-}p \rightarrow \nu_e Hj$

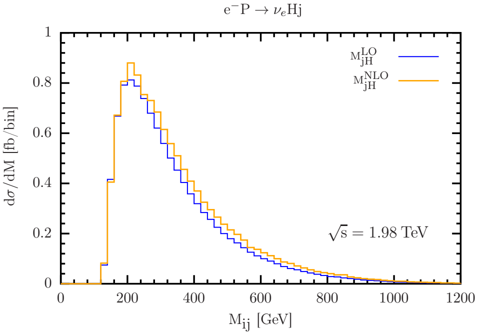

Figure: The NLO differential cross section distribution with respect to invariant masses ($M_{ij/ijk}$).

Outlook

Anomalous $HVV(V = W^{\pm}, Z)$ coupling

Most general Lagrangian

$$g\left(m_W \kappa_W W^+_\mu W^{-\mu} + \frac{\kappa_Z}{2\cos\theta_W} m_Z Z_\mu Z^\mu\right) H$$

$$-\frac{g}{m_W}\left[\frac{\lambda_{1W}}{2} W^{+\mu\nu} W^-_{\mu\nu} + \frac{\lambda_{1Z}}{4} Z^{\mu\nu} Z_{\mu\nu}\right.$$

$$+\lambda_{2W}(W^{+\nu}\partial^\mu W^-_{\mu\nu} + h.c.) + \lambda_{2Z} Z^\nu \partial^\mu Z_{\mu\nu}$$

$$\left.+\frac{\tilde{\lambda}_W}{2} W^{+\mu\nu}\widetilde{W}^-_{\mu\nu} + \frac{\tilde{\lambda}_Z}{4} Z^{\mu\nu}\widetilde{Z}_{\mu\nu}\right] H$$

$g \rightarrow SU(2)$ coupling parameter

$$\tilde{V}^{\mu\nu} = \frac{1}{2}\epsilon^{\mu\nu\alpha\beta} V_{\alpha\beta}$$

$$V^{\mu\nu} = \partial^\mu V^\nu - \partial^\nu V^\mu$$

Outlook

Anomalous $HVV(V = W^{\pm}, Z)$ coupling

Most general Lagrangian

$$g\left(m_W\kappa_W W_\mu^+ W^{-\mu} + \frac{\kappa_Z}{2\cos\theta_W} m_Z Z_\mu Z^\mu\right) H$$

$$-\frac{g}{m_W}\left[\frac{\lambda_{1W}}{2} W^{+\mu\nu} W^-_{\mu\nu} + \frac{\lambda_{1Z}}{4} Z^{\mu\nu} Z_{\mu\nu}\right.$$

$$+\lambda_{2W}(W^{+\nu}\partial^\mu W^-_{\mu\nu} + h.c.) + \lambda_{2Z} Z^\nu \partial^\mu Z_{\mu\nu}$$

$$\left.+\frac{\tilde{\lambda}_W}{2} W^{+\mu\nu}\widetilde{W}^-_{\mu\nu} + \frac{\tilde{\lambda}_Z}{4} Z^{\mu\nu}\tilde{Z}_{\mu\nu}\right] H$$

SM like

CP even

Derivative of fields

CP odd

Outlook

Results and discussion

Observables: $|\Delta\phi|$ is azimuthal correlation of two particles 1 and 2

$$|\Delta\phi| = cos^{-1}(\hat{p}_{T1} \cdot \hat{p}_{T2})$$

Motivation: $|\Delta\phi|$ distribution is a good observable to distinguish CP-even and CP-odd couplings of CC process considered in ref. [2]

Ref. [2]: Phys. Rev. Lett. 109 (2012) 261801, [1203.6285]

Outlook[2]

Results

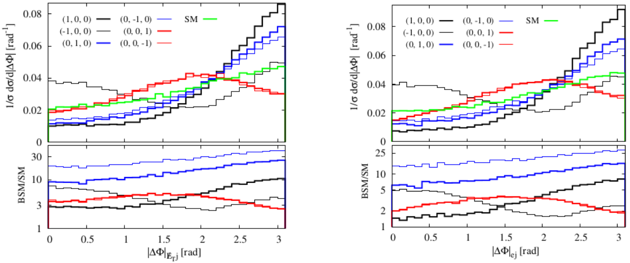

BSM effects in $|\Delta\phi|$ distribution for CC (left) and NC (right)

$(\lambda_{1V}, \lambda_{2V}, \widetilde{\lambda}_V)$

- $|\Delta\phi|$ is sensitive to individual effect of new couplings
- Deviation in distribution with respect to SM is largest for λ_{2V} and smallest for $\widetilde{\lambda}_V$

[2] **Pramod Sharma and Ambresh Shivaji, JHEP10(2020)108.**

Summary

- We have computed the QCD NLO correction to H production with one jet at eP collider.
- We found the NLO QCD correction around 10% at 1.98 TeV CME.
- We found that the invariant mass and the p_T distributions are harder with NLO corrected results.
- $|\Delta_\phi|$ distribution is sensitive to HVV ($V = W^\pm, Z$) coupling.
- We are motivated to see the effect of effective couplings for NLO corrected results at HVV vertex within the experimental uncertainty.

Thank You